Developmental Biology 382 (2013) 48–56

Contents lists available at ScienceDirect

Developmental Biology

journal homepage: www.elsevier.com/locate/developmentalbiology

Rebuilding MTOCs upon centriole loss during mouse oogenesis

Małgorzata Łuksza [a,b], Isabelle Queguigner [a,b], Marie-Hélène Verlhac [a,b,*], Stéphane Brunet [a,b,*]

[a] Collège de France, Center for Interdisciplinary Research in Biology, CIRB, UMR CNRS 7241/INSERM-U1050, Equipe Labellisée Ligue Contre le Cancer, 11 place Marcelin Berthelot, 75005 Paris, France
[b] Memolife Laboratory of Excellence and Paris Science Lettre, France

ARTICLE INFO

Article history:
Received 23 September 2012
Received in revised form
25 July 2013
Accepted 30 July 2013
Available online 14 August 2013

Keywords:
Oogenesis
Mouse
Growth phase
Acentriolar MTOC
NEBD

ABSTRACT

The vast majority of animal cells contain canonical centrosomes as a main microtubule-organizing center defined by a central pair of centrioles. As a rare and striking exception to this rule, vertebrate oocytes loose their centrioles at an early step of oogenesis. At the end of oogenesis, centrosomes are eventually replaced by numerous acentriolar microtubule-organizing centers (MTOCs) that shape the spindle poles during meiotic divisions. The mechanisms involved in centrosome and acentriolar MTOCs metabolism in oocytes have not been elucidated yet. In addition, little is known about microtubule organization and its impact on intracellular architecture during the oocyte growth phase following centrosome disassembly. We have investigated this question in the mouse by coupling immunofluorescence and live-imaging approaches. We show that growing oocytes contain dispersed pericentriolar material, responsible for microtubule assembly and distribution all over the cell. The gradual enlargement of PCM foci eventually leads in competent oocytes to the formation of big perinuclear MTOCs and to the assembly of large microtubule asters emanating from the close vicinity of the nucleus. Upon meiosis resumption, perinuclear MTOCs spread around the nuclear envelope, which in parallel is remodelled before breaking-down, via a MT- and dynein-dependent mechanism. Only fully competent oocytes are able to perform this dramatic reorganization at NEBD. Therefore, the MTOC-MT reorganization that we describe is one of key feature of mouse oocyte competency.

Introduction

In most animal cells, canonical centrosomes are the main organizers of the microtubule cytoskeleton. They are composed of a pair of centrioles surrounded by proteinaceous material (PCM for PeriCentriolar Material). The PCM nucleates microtubules and controls their spatial organization, by tethering their minus-ends. As a consequence, in many non-polarized cells, centrosomes are essential for the accurate positioning of the nucleus and organelles and therefore for the general intracellular architecture (Bornens, 2008). During cell division, they are key players in the formation of a bipolar spindle. In addition, by monitoring spindle position, they contribute to the geometry of division (Thery and Bornens, 2006).

In most species, oogenesis, the process which gives rise to female haploid gametes or eggs, is associated with centrioles loss and centrosome disassembly. The molecular bases of this phenomenon remain unknown (Manandhar et al., 2005). The exact stage at which it occurs varies across species and in mammals remains poorly characterized. Electron microscopy analysis performed on human ovaries suggests that centrioles are already absent at early oogenesis, *i.e.* in oocytes enclosed in primordial follicles (Hertig and Adams, 1967). Centrosome loss is reversed after fertilization and canonical centrosomes reassemble in the zygote or in the embryo. This process depends on the contribution of sperm-associated centrioles in many species, with the exception of rodents. In mouse, the sperm centriole degenerates after fertilization and *de novo* assembly only begins around the 64-cells stage embryo via unknown mechanisms (Gueth-Hallonet et al., 1993).

During oogenesis, mammalian oocytes are enclosed in ovarian follicles, and both oocyte and follicle develop in a synchronous fashion (for review, see (Edson et al., 2009). Following centriole elimination, oocytes are arrested in diplotene of the first meiotic prophase (corresponding to a G2 arrest of the cell cycle) and can be cyclically recruited to a protracted growth phase. During this critical phase, oocytes acquire the ability to resume meiosis, get fertilized and give rise to developing embryos. Morphologically, their size increases dramatically: in mouse, oocyte diameter rises

* Corresponding authors at: Collège de France, Center for Interdisciplinary Research in Biology, CIRB, UMR CNRS 7241/INSERM-U1050, Equipe Labellisée Ligue Contre le Cancer, 11 place Marcelin Berthelot, 75005 Paris, France.
E-mail addresses: marie-helene.verlhac@college-de-france.fr (M.-H. Verlhac), stephane.brunet@inserm.fr (S. Brunet).

0012-1606/$ - see front matter © 2013 Elsevier Inc. All rights reserved.
http://dx.doi.org/10.1016/j.ydbio.2013.07.029

from 10 to 85 μm (Krarup et al., 1969). In parallel, the intracellular architecture is remodelled. The nucleus in particular becomes relocated from the periphery to the central area of the cell (Brunet and Maro, 2007). Oocytes that have successfully completed growth – *i.e.* competent oocytes – can enter meiotic maturation and be ovulated: they undergo asymmetric divisions and form a large and haploid egg, ready for fertilization, and tiny polar bodies that eventually degenerate.

Dividing eggs contain discrete and numerous structures defined biochemically by two major PCM components, pericentrin and γ-tubulin. During meiotic spindle formation, they are progressively sorted and clustered to the spindle poles where they act as MTOCs (for Microtubule Organizing Centers (Carabatsos et al., 2000; Gueth-Hallonet et al., 1993; Szollosi et al., 1972). These MTOCs do not nucleate astral microtubules, in contrast to canonical centrosomes, and this property contributes to minimize the size of the polar body (Verlhac et al., 2000). Centriole elimination during oogenesis may thus be considered as a strategy to maximize the asymmetry of egg division and generate a unique large cell competent for fertilization (for review, see (Brunet and Verlhac, 2011). The origin of these acentriolar MTOCs remains controversial. Initially thought to be present and active in prophase arrested oocytes (Mattson and Albertini, 1990; Can et al., 2003), they have been more recently proposed to form at the onset of the first meiotic division only, either through microtubule self-organization mechanisms (Schuh and Ellenberg, 2007), or via the activation of large and quiescent structures assembled in prophase-arrested oocytes (Calarco, 2000).

To tackle this issue, we investigated the microtubule-MTOCs organization throughout the oocyte growth phase and meiosis resumption by coupling immunostaining and live-imaging approaches. We show that upon centriole loss, growing oocytes contain dispersed PCM foci responsible for microtubule assembly and random distribution all over the cell. The gradual enlargement of these foci and their progressive concentration at the nuclear envelope leads, at the end of the growth phase, to the remodelling of the microtubule network into predominant large asters irradiating towards the cell periphery. This MTOC-microtubule organization in competent oocytes mainly appears to prepare the nucleus to the final entry into meiotic divisions. Meiosis resumption is indeed associated with a microtubule- and dynein-dependent redistribution of perinuclear MTOCs along the nuclear envelope. This process induces a reshaping of the nuclear envelope prior to NEBD and ends up by an isotropic repartition of MTOCs around condensed chromosomes, a configuration which may facilitate MTOCs parititioning at early steps of bipolar spindle assembly.

Materials and methods

Mouse oocyte collection, culture and microinjection

Oocytes were collected from 11-week-old OF1 females from secondary (preantral, a mid stage of growth) and tertiary (antral) follicles. Secondary follicles were recovered and subsequently shortly incubated in an M2+BSA medium supplemented with 0.25% pronase (B grade Calbiochem) to facilitate the mechanical disruption of the follicle. Oocytes liberated from tertiary follicles were collected as previously described (Brunet and Maro, 2007). The collected oocytes were further separated according to their to size and the morphology of their *zona pellucida* (ZP) *i.e.* the glycoprotein envelope enclosing the oocyte. Smaller oocytes exhibiting a tightly associated and rough ZP were separated from large oocytes with a smooth ZP. Eventually, their chromatin configuration was analyzed by immunofluorescence or live imaging studies. From the pool of large oocytes, only cells with nucleoli fully surrounded by chromatin rings were analysed and classified as "competent". From the pool of small oocytes only the ones characterized by non-surrounded nucleoli were considered and classified as "incompetent oocytes" (Mattson and Albertini, 1990).

Oocytes were cultured in M2+BSA medium supplemented with 1 μM dbc-AMP (Sigma) to prevent meiotic maturation.

Microinjections were performed using a FemtoJet microinjector (Eppendorf). Following injection, oocytes were left for 1–2 h to allow expression of exogenous proteins from cRNAs prior to imaging.

Plasmid collection and in vitro transcription of synthetic RNA

We used the previously described constructs: pRN3-EB3-GFP (Breuer et al., 2010), pRN3-YFP-Rango-CFP (Dumont et al., 2007a), pRN3-histone-RFP (Tsurumi et al., 2004), pspe3-GFP-Utr (Azoury et al., 2008), pspe3-Venus-Plk1 (Kolano et al., 2012). Rango was also subcloned into pspe3-mCherry. *In vitro* synthesis of capped cRNAs was performed using mMessage mMachine T3 kit (Ambion) as previously described (Verlhac et al., 2000).

Immunofluorescence

For microtubule analysis, oocytes were fixed using glutaraldehyde as previously described (Brunet et al., 1999). We used a rat monoclonal antibody against tyrosinated α-tubulin (YL1/2, Abcam) at 1:200. For MTOC analysis, oocytes were fixed using paraformaldehyde as in (Dumont et al., 2007a). Monoclonal anti-pericentrin (BD, at 1:400) and/or polyclonal anti γ-tubulin (Abcam at 1:800) were used. After primary antibodies incubation and subsequent washes, oocytes were labelled with the corresponding secondary antibodies (Jackson ImmunoResearch Laboratories, Inc.). Chromatin was labelled with 5 μg/ml Hoechst (Invitrogen)

Images were acquired using a Leica SP5 confocal microscope using a Plan APO 63 × /1.25 NA objective or, in the case of Supplementary Fig. 2B, with a Leica SP8 Gated STED confocal microscope. Z-series were performed with Z-steps between 0.4 and 0.7 μm.

Videomicroscopy

For time-lapse imaging, oocytes were enclosed in a thermostatic chamber (Life Imaging Services) at 37 °C in M2+BSA medium supplemented with dbcAMP. Histone-RFP, EB3-GFP, YFP-Rango, Rango-mCherry, Venus-Plk1 and GFP-Utr expressing cells were imaged using a Photometrics CCD camera (Coolsnap HQ2) mounted on a Leica DMI6000B microscope coupled to a Sutter filter wheel (Roper Scientific) and a Yokogawa CSU-X1-M1 spinning disk using a Leica HC Plan-APO 40 × /1.25 NA objective.

Image analysis

To estimate the size of individual MTOCs in fixed oocytes, confocal Z-series were acquired with a Z-step of 0.8 μm and maximum projections of Z planes were performed. The resulting pericentrin signal was binarized and the area (μm^2) was calculated using Image J (National Institute of Health).

For microtubule dynamics, time-lapse images were taken at 1 s intervals for 1 min. Tracking of individual microtubules was performed using MTrackJ plugin (Biomedical imaging group Rotterdam) in Image J. For nuclear centroid movement and circularity analysis, time-lapse images were taken at 30 s intervals during 10 min and time-stacks were aligned based on the GFP-Utr cortical staining. The position of the centroid was automatically tracked in Metamorph (Universal Imaging). The circularity of nuclei was extracted in Image J (NIH). For the measure of YFP-Rango leaking

at NEBD, oocytes were imaged every 4 min for 2 h. NEBD was scored in bright-field and fluorescence analysis was subsequently performed from 7 time-points preceding nuclear breakdown. The intensity of YFP-Rango was measured from 4 different regions of the cytoplasm in Metamorph (Universal Imaging) and the average intensity was plotted against time-to-NEBD. To follow MTOCs at NEBD, cells blocked in prophase I were injected with Venus-Plk1 and Histone-RFP and incubated for 1 h in medium, supplemented or not with either 50 μM Ciliobrevin D (Calbiochem) or 1 μM Nocodazole (Sigma). After incubation dbc-AMP was washed out and the cells were imaged every 8 min for 2 h. Data were processed and statistical analyses were performed using Excel (Microsoft) and Prism (GraphPad Software, inc) softwares.

Results

Oocyte growth is characterized by MTOC-microtubule remodelling

MTOC-microtubule organization was first investigated by immunostaining of oocytes collected at 3 representative stages of growth phase. Mid-growth was epitomized by preantral oocytes recovered from secondary follicles. The last steps of growth were represented by incompetent and competent oocytes, both recovered from antral follicles. Competent oocytes are the only ones able to resume meiosis, undergo meiotic divisions and fertilization (Krarup et al., 1969).

In both preantral and incompetent oocytes the microtubule meshwork filled the whole cytoplasm (Fig. 1A). Few dispersed and small-sized PCM foci, defined by pericentrin and γ-tubulin co-labelling (Fig. S1A), were present, each of them poorly connected to microtubules. In addition, small astral-like microtubule structures unconnected to visible PCM could be observed, suggesting the existence of smaller PCM undetected by immunostaining (Fig. 1A). In striking contrast, in competent oocytes, microtubules exhibited a predominant astral arrangement with large PCM foci at their hub. Microtubule asters were mostly associated with the nucleus surface (Fig. 1A).

The morphological changes of PCM foci during oocyte growth were quantified. The number of visible foci remained globally stable, reaching an average of 3 in competent oocytes. The foci underwent a 5-fold increase in size, starting with a mean value of 0.5 μm^2 in preantral oocytes and reaching 2.8 μm^2 in competent ones (Fig. 1B). Large PCM foci appeared like alveolated structures at high resolution (Fig. S2). Eventually, while more than 60% of the visible foci were clustered at the cortex of preantral and incompetent oocytes, they were predominantly associated with the nucleus in mature oocytes (Fig. 1B).

Microtubules gain astral pattern at the end of the growth phase

Microtubules are dynamic structures. We thus turned to live imaging of oocytes expressing a GFP tagged version of EB3 (for End Binding protein 3), a marker of microtubule (+) ends (Stepanova et al., 2003), to better understand their global organization during oocyte growth.

At each growth stage, individual EB3-GFP comets could be tracked for several seconds, indicative of a relative stability expected for interphasic microtubules (Desai and Mitchison, 1997). The growth speed of individual microtubules was measured (Table 1): at the exception of a significant but modest increase between preantral and incompetent oocytes ($P < 0.0001$ Student's t test), this parameter

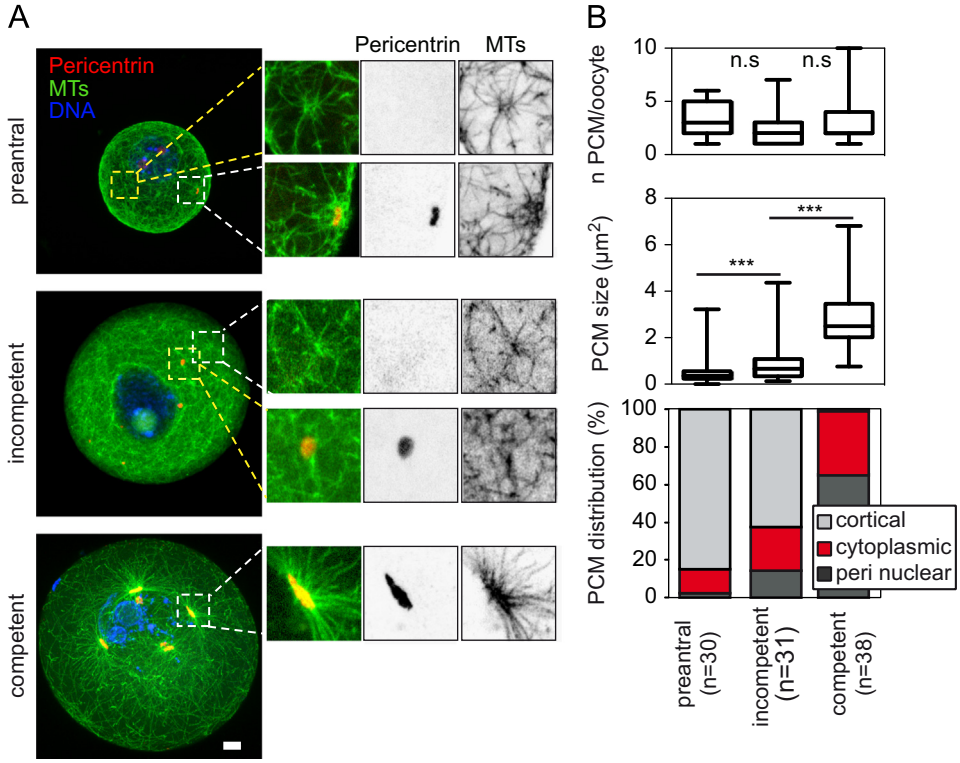

Fig. 1. MTOC-Microtubule network is remodelled during oocyte growth. (A) Immunofluorescence of oocytes collected at the indicated stages of growth. Z-projections of microtubules (in green), PCM foci (in red) and chromatin (in blue) of whole oocytes are presented. Scale bar is 10 μm. Insets present magnified views of the specified areas on selected stacks: overlay appears left, pericentrin and microtubule stainings appear in the middle and right respectively. (B) PCM morphological changes during oocyte growth. (Upper graph) Whiskers box plot representation of the total number of visible PCM foci per oocyte in preantral, incompetent and competent oocytes. (Middle graph) Whiskers box plot representation of the size of individual pericentrin foci (estimated in μm^2) at the indicated growth stages (***, $P < 0.0001$, Mann Withney test). (Lower graph) PCM foci progressively associate with the nucleus. Distribution of PCM foci between the cortical (light grey), cytoplasmic (red) and perinuclear (dark grey) compartments of the oocyte at the indicated growth stages. For each group, the number of oocytes analyzed (n) is indicated in brackets.

remained unchanged around 16 μm min^{-1}. The regime of microtubule dynamics was thus stable during oocyte growth.

In preantral and incompetent oocytes, microtubules grew all over the cytoplasm, and the projections of EB3-EGFP of long time-lapse sequences did not reveal any clear microtubule pattern, in contrast with the astral structures present in competent oocytes (Fig. 2A). We then analyzed the directionality of growing microtubules using a 7 μm wide cortical layer of the cytoplasm. In preantral and incompetent oocytes, equivalent amounts of microtubules were found to grow towards the periphery, inwards or parallel to the oocyte surface (Fig. 2B,C), indicating no preferential growth direction at that stages. In contrast, microtubules were predominantly growing outwards in competent oocytes (Fig. 2C).

In parallel, the sites of microtubule nucleation were explored using classical microtubule regrowth assays. To do so, microtubules were fully depolymerised by incubating oocytes in cold medium for 1 h. They were then let to regrow at 37 °C for 2 min. Cells were fixed, microtubules and PCM were analyzed by immunofluorescence. In both preantral and incompetent oocytes, microtubule asters, with PCM foci at their hub were observed in the cytoplasm (Fig. 3A). The number of emanating microtubules was correlated with the foci size (Fig. 3B). More foci – in average ten per oocyte – were observed compared to untreated oocytes. This was reminiscent of asters self-organization described in *Xenopus* egg extracts (Verde et al., 1991) and in mouse eggs (Maro et al., 1985) and unveiled the presence of small PCM foci dispersed in the cytoplasm in growing oocytes that were not detected initially using immunostaining approaches at steady state. In competent oocytes, the majority of microtubules emanated from large PCM foci, reminiscent in size and number of the structures observed in untreated oocytes (Fig. 3A). Their relatively high nucleation capacity was correlated with their size (Fig. 3B). The γ-tubulin/pericentrin ratio measured on individual PCM foci was not significantly different between growing and competent oocytes (Fig. 3C). The relative PCM composition might be stable during the growth phase and the increase in nucleation capacity could to some extent be due to enlargement of the structures.

Taken together these results indicate that oocyte growth is associated with a major remodelling of the MTOC- microtubule network. During most of the protracted growth phase following centriole loss, oocytes do contain multiple dispersed PCM foci responsible for microtubule distribution all over the cell. Upon gradual PCM reorganization, microtubules gain a robust astral organization at the end of the growth phase. They mostly emanate from large PCM foci concentrated on the nucleus surface and grow radially towards the cell cortex.

Table 1
Variation of microtubule growth speed during oocyte growth phase.

Preantral	Incompetent	Competent
14.2 ± 2	17.3 ± 2	16.5 ± 2

Mean and standard deviation are reported (μm min^{-1}) (n=50 microtubules from 5 individual oocytes in each category).

Microtubules reorganization increases nucleus malleability in competent oocytes

How does such MTOC-microtubule remodelling impact the intracellular architecture of growing oocytes? The end of growth phase is characterized by a relocation of the nucleus from the periphery toward the centre of the cell (Bellone et al., 2009; Brunet and Maro, 2007). Since in many cell systems, including *Drosophila* oocyte, microtubules are key players in nucleus positioning (Bornens, 2008; Zhao et al., 2012), we investigated their potential contribution

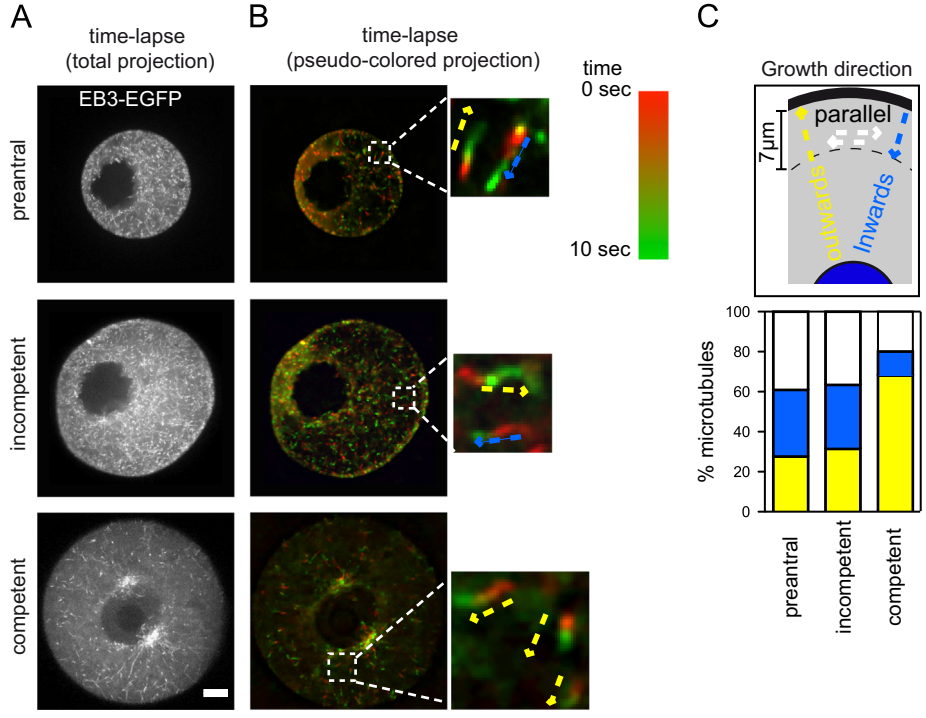

Fig. 2. Microtubule dynamic organization during oocyte growth. (A) Maximum intensity projection of EB3-GFP time-lapse sequences (55 frames spaced every second) is presented to visualize the general microtubule organization in oocytes at the indicated stage of growth. Scale bar is 10 μm. (B) Ten seconds time-lapse sequences were pseudo-coloured according to the indicated green-to-red LUT in order to depict microtubule directionality in oocytes presented in A (microtubule grow "from red to green"). Insets: magnified views of selected areas. Blue and yellow arrows indicate inwards and outwards growth directions respectively. (C) Quantification of microtubule directionality using the pseudo-coloured images. For each category of oocytes, inwards (blue) and outwards (yellow) growing microtubules as well as microtubule running parallel to the cortex (white) were counted in a 7 μm wide layer of cytoplasm. In preantral oocytes: 327 growth events were counted in 4 oocytes. In incompetent oocytes: 303 events were counted in 5 oocytes. In competent oocytes 306 events were counted in 5 oocytes.

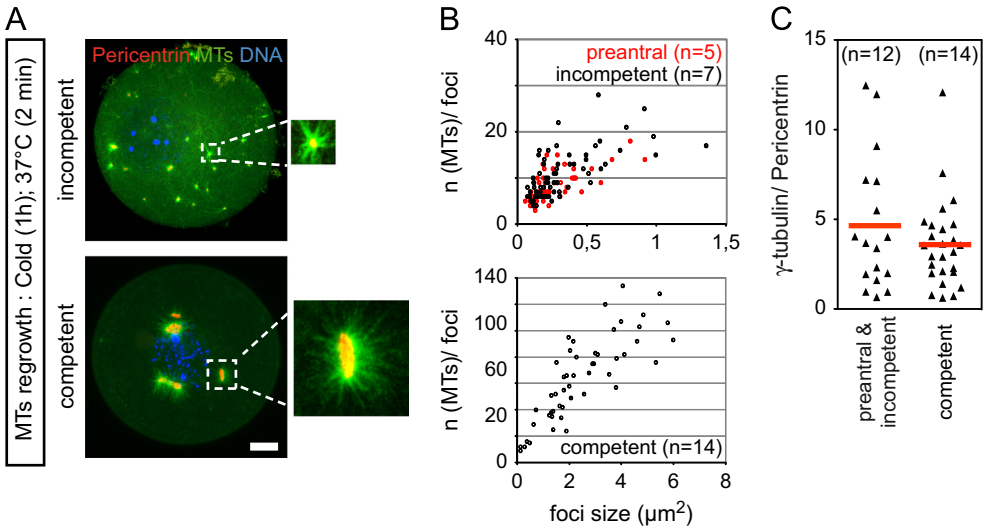

Fig. 3. MTOC nucleation activity increases during oocyte growth. (A) Microtubule nucleation was assessed using classical microtubule regrowth assays. Microtubules were depolymerised by incubating oocytes in cold medium for 1 h. They were then let to regrow at 37 °C for 2 min. Cells were fixed and analyzed by immunostaining. Representative Z-projections of microtubules (green), pericentrin (red) and chromatin (blue) of oocytes are presented. Incompetent and competent oocytes appear in top and bottom row respectively. Scale bar is 10 μm. White Insets present magnified view of selected microtubule asters. (B) Estimation of the nucleation activity. For each individual foci, the number of microtubules is plotted against its size (area in μm^2). First graph presents the measures performed in preantral (red circles) and incompetent oocytes (black circles). Second graph presents the measures in competent oocytes. (C) γ-tubulin levels on PCM foci are stable during oocyte growth. γ-tubulin and pericentrin levels on individual PCM foci were quantified in preantral and incompetent *versus* competent oocytes. For each group, the number of oocytes analyzed is indicated. Ratios of integrated intensities for individual PCM foci are presented. Red bars represent mean values. (non significant, $P=0.6$; Mann Withney test).

to nucleus centring in our model. High doses of microtubule poison have been documented to displace the nucleus from the centre to the cell periphery in competent oocytes (Alexandre et al., 1989). Nevertheless, using more physiological conditions *i.e.* 1 μM of Nocodazole, we did not observe any global nucleus movement neither in incompetent nor in competent oocytes (data not shown). This indicated that microtubules are not essential for maintenance of the nucleus in its central location.

Live imaging of nucleus and cell contours (Fig. 4A), respectively visualized with YFP-Rango (for Ran-regulated Importin ß cargo (Dumont et al., 2007a; Kalab et al., 2002)) and GFP-Utr (for Utrophin (Azoury et al., 2008; Burkel et al., 2007)), revealed that the nucleus was a dynamic and malleable object (Fig. 4B). To quantify this phenomenon, we tracked its centroid over time and analysed its maximum displacement. This parameter increased more than 2-fold between incompetent and competent oocytes (Fig. 4C). This leap coincided with the acquisition of perinuclear microtubule asters, suggesting that these structures can actively impact the nucleus. Indeed, nuclear centroid displacement was reduced upon microtubule depolymerization (Fig. 4C). Moreover, numerous curved microtubules were observed to intrude invaginations at the nuclear surface (Fig. 4D). Furthermore, in control oocytes, the nucleus circularity was variable over a time course of 10 min (Fig. 4E, top panel and black curve). Over the same time frame, the curves corresponding to nuclear outlines could not be superimposed (Fig. 4F top panel) and the variation of nuclear circularity was high as observed on many oocytes (Fig. 4G). These data were indicative of local and dynamic deformations of the nuclear surface. The variations measured were totally suppressed upon microtubule depolymerization (Fig. 4E, bottom panel and red curve, F, bottom panel and G) showing they were microtubule -dependent.

Therefore, the acquisition in competent oocytes of large microtubule perinuclear asters impacts a malleable nuclear envelope by establishing local and dynamic deformations.

Reorganizing MTOC and microtubules prior to meiotic division

We reasoned that the establishment of microtubule-dependent dynamic deformations of the nuclear envelope in competent oocytes could serve to prepare meiosis resumption and promote nuclear envelope breakdown. To test this hypothesis, we first investigated whether perturbation of microtubules could impact the timing of nuclear envelope breakdown. As previously shown, the nucleus starts to leak before detection of its breakdown by bright-field microscopy (Azoury et al., 2011). This leak can be monitored using the nuclear Rango probe. Upon Nocodazole or Ciliobrevin-D (Dynein inhibitor; (Firestone et al., 2012)) treatment, the kinetics of nucleus permeabilization were very modestly retarded (Fig. S3A,B), suggesting that microtubules and Dynein activity are dispensable for timely meiosis resumption.

Using Venus-Plk1 to visualize MTOCs (Kolano et al., 2012), we then followed the dynamic behaviour of MTOCs in live from oocytes released of the block in prophase I and undergoing NEBD. In parallel, MTOC organization was analyzed at NEBD by immunostaining. NEBD could be observed in bright-field around 1.5 h after the release from the dbcAMP block (Fig. 5A, upper row). Nevertheless, as previously observed, 25 min before this event, the nucleus started to become permeable as indicated by the release of the nuclear probe YFP-Rango into the cytoplasm (Fig. S3A,B). Concomitantly MTOCs reorganized: prior to NEBD, the globular structures present in prophase I started to elongate on the nucleus surface. At NEBD, they fragmented into small units that eventually surrounded the condensed chromosomes (Fig. 5A, upper row and Fig. 5B, top panel). Interestingly, the ability of MTOCs to undergo such a spectacular reorganization at NEBD was an attribute of fully competent oocytes. Indeed, it was never observed in oocytes that were able to undergo NEBD but remained blocked in meiosis 1 (refered as partially competent in the literature (Sorensen and Wassarman, 1976)). MTOC elongation and fragmentation in competent oocytes were strictly abolished when they underwent NEBD in the presence of 1 μM Nocodazole (Fig. 5A, middle row and 5B). Upon inhibition of Dynein using Ciliobrevin D at 50 μM, MTOCs started to elongate but failed to fragment into small units (Fig. 5A, lower row). Instead large stretches of PCM were observed at NEBD (Fig. 5B).

Therefore, meiosis resumption and NEBD are associated with a perinuclear MTOCs reorganization from large globular into punctuate structures that evenly surround the condensed chromosomes. This reorganization is microtubule- and Dynein-dependent.

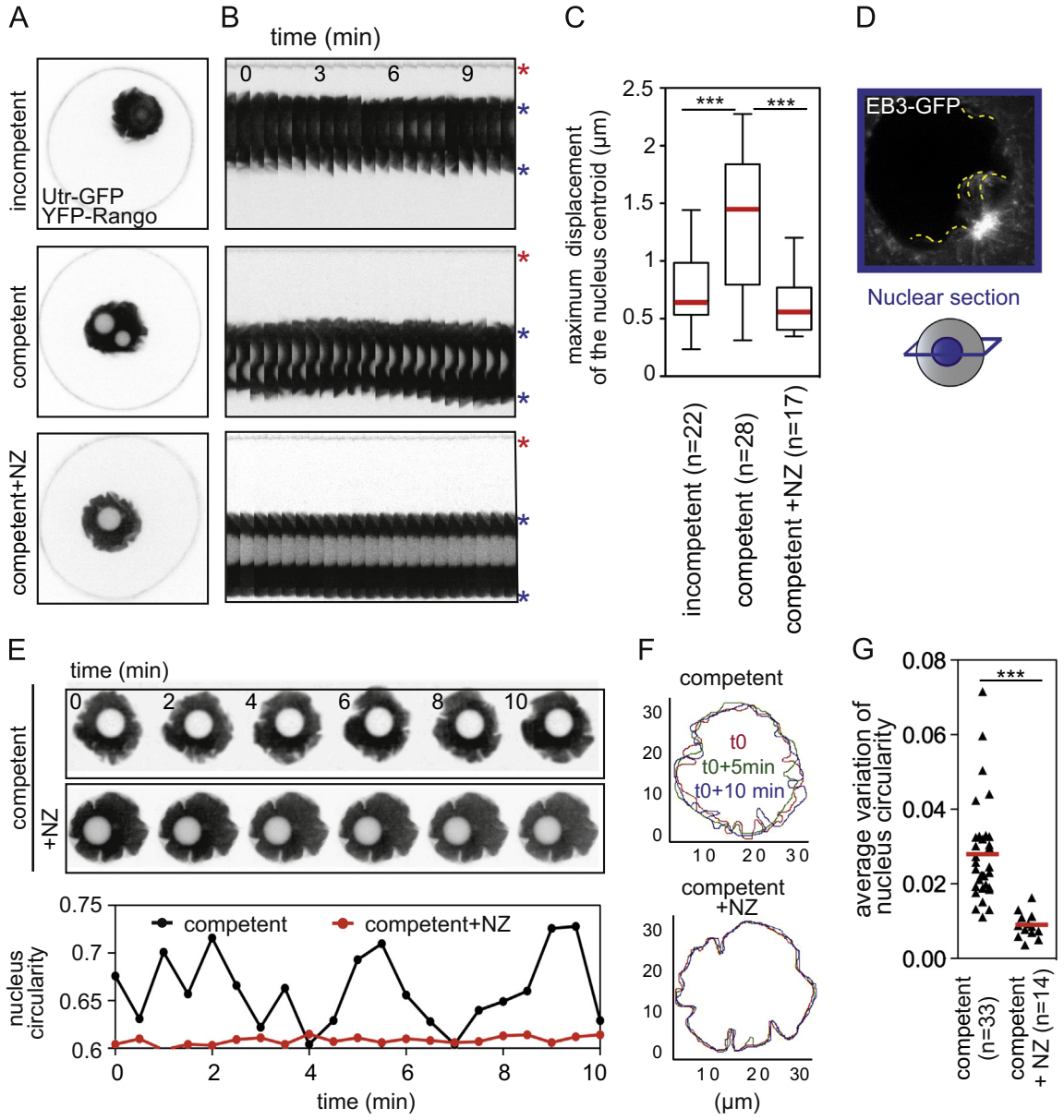

Fig. 4. MTOC- microtubule remodelling impacts a malleable nucleus. (A) YFP-Rango and GFP-Utr probes were used to visualize nucleus and oocyte contours respectively. Representative image of oocytes: incompetent (upper panel), competent (middle panel) and competent incubated for 1 h in 1 μM Nocodazole (lower panel). (B) Kymographs of nucleus motility in the corresponding oocytes. On the left, nucleus and cell boarders are indicated by blue and red asterisks respectively. Time points are indicated. Scale bar is 5 μm. (C) Competent oocytes exhibit increased motility compared to incompetent ones. This motility is reduced upon microtubule depolymerization. Whiskers box plot representation of the maximum amplitude of nucleus centroid displacements (in μm) calculated for each cell. For each group, the number of oocytes analyzed is indicated. Median appears as red bar (***, $P < 0.0001$, t test). (D) Microtubules were tracked using EB3-GFP for a nuclear section (blue square) of the oocyte. The maximum intensity projection from 10 s time-lapse sequences is presented. Microtubules of interest are underlined with yellow dashed lines. (E) Nocodazole strongly inhibits the dynamics of nuclear invaginations in competent oocytes. YFP-Rango probe was used to visualize the nucleus in competent (upper gallery) and Nocodazole-treated competent oocytes (lower gallery) during 10 min long sequences. For each condition, the circularity shape factor of the nucleus is plotted against time (time scale in minutes). (F) Representation of nuclear invagination changes for competent oocytes treated or not with Nocodazole. Red, green and blue lines show the outline of the nucleus at time intervals of 5 min. (G) Analysis of variations of the nucleus circularity shape factor in individual cells from groups of untreated or Nocodazole treated competent oocytes. For each group, the number of oocytes analyzed is indicated. Median appears as red bar (***, $P < 0.0001$, t test with Welsh correction).

We then analyzed the nucleus shape in live during the 1.5 h preceding NEBD. Initially, the whole surface of the nucleus was covered by numerous invaginations (Fig. 5C; see also Fig. 4D). Around 60–50 min before NEBD, the majority of these invaginations started to disappear such that the nuclear surface smoothened. Only one or few enlarged invaginations persisted (Fig. 5C, upper row). The smoothening of nuclear surface was abolished in Nocodazole-treated oocytes (Fig. 5C, lower row). The co-injection of Rango-mCherry and Venus-Plk1 revealed that MTOCs were elongating along the remaining invaginations (Fig. 5D).

These observations indicate that the MTOC-microtubules reorganization drives an intense remodelling of the nucleus surface preceding NEBD.

Discussion

In mammals, oogenesis is associated with early centriole elimination. Yet, at the end of oogenesis, dividing eggs have acquired functional acentriolar MTOCs that shape meiotic spindle

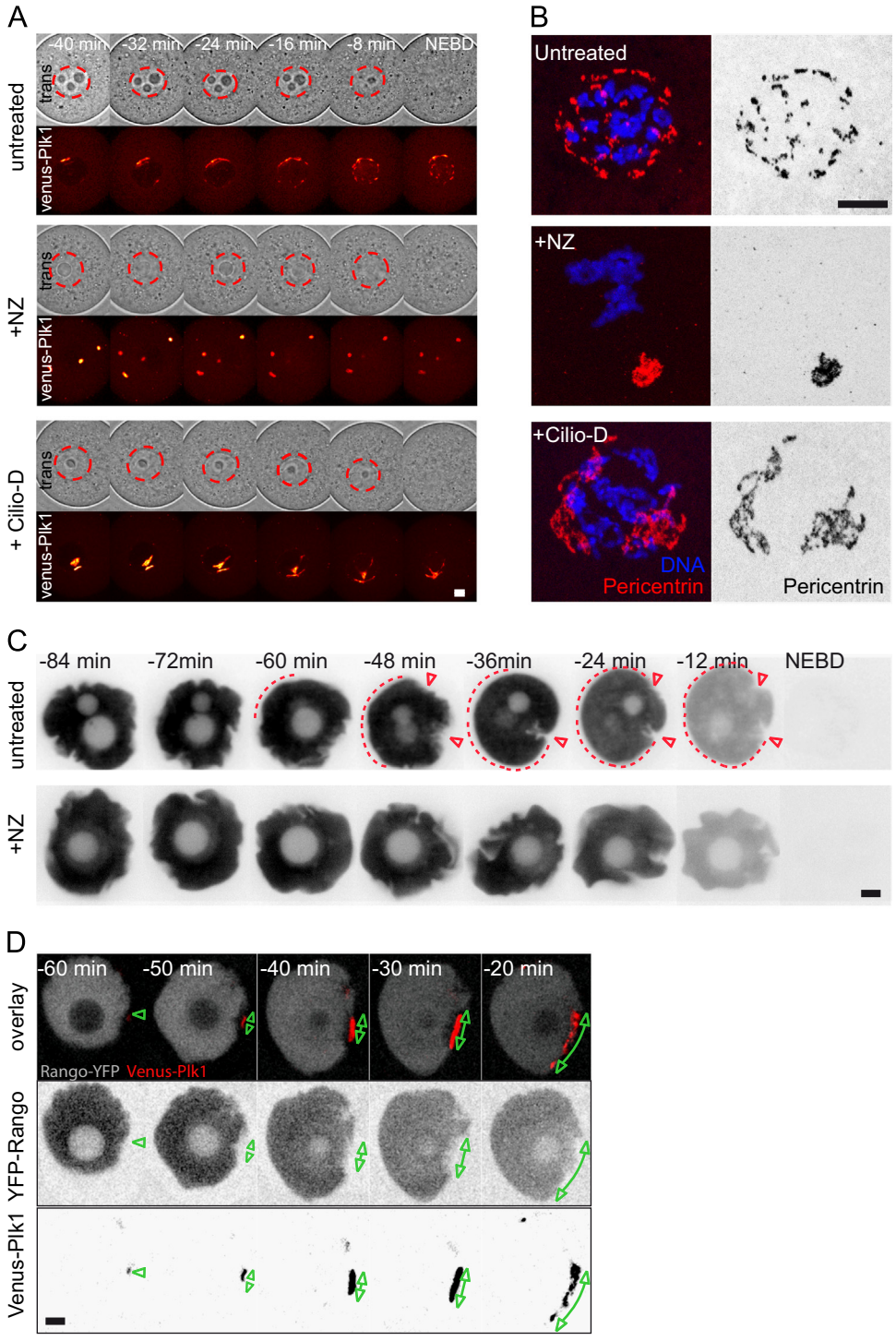

Fig. 5. MTOCs redistribution at meiosis onset depends on MTs and Dynein. (A) MTOC redistribution at meiosis 1 onset. Venus-Plk1 was used to visualize MTOC dynamics in live. For each condition *i.e.* untreated competent oocytes (upper panel, $n=18$); Nocodazole-treated (NZ; middle panel, $n=16$) or Ciliobrevin-D (Cilio-D, lower panel, $n=19$) competent oocytes, transmitted light pictures are presented with the corresponding fluorescent images. Time is indicated relative to the time of NEBD, as observed by bright-field. Scale bar is 10 μm. (B) Immunofluorescence of oocytes collected around NEBD in the indicated conditions *i.e.* untreated, Nocodazole or Ciliobrevin-D treated competent oocytes. Z-projections of PCM foci (in red) and chromatin (in blue) from whole oocytes are presented. Scale bar is 10 μm. Corresponding pericentrin staining is presented in the right column. (C) YFP-Rango was used to follow the nucleus in live during meiosis 1 onset in competent untreated (upper panel; $n=33$) and Nocodazole-treated (lower panel; $n=46$) oocytes. Time is indicated relative to NEBD. Major invaginations are indicated by red triangles. Dashed red lines indicate the smooth areas of the nucleus. Scale bar is 5 μm. (D) MTOCs elongate with time within the invaginations. Time is indicated relative to NEBD. YFP-Rango appears in grey and Venus-Plk1 in red in the overlay gallery. In the Rango and Plk1 galleries, green arrows indicate the position of elongating MTOCs. Scale bar is 5 μm. 31 MTOCs were analyzed in 23 oocytes.

poles (Dumont and Desai, 2012). To better understand the origin of these acentriolar structures, we focused our attention on the microtubule-MTOCs organization throughout the preceding oocyte growth phase.

We show that during most of this phase following centriole elimination, oocytes contain small-sized PCM foci dispersed within the cell that support microtubule assembly. Microtubules irradiate within the whole cytoplasm without any preferential

directionality. As a consequence the microtubule network appears loosely organized. It is only at the end of the growth phase – when oocytes have gained the ability to undergo meiotic divisions and fertilization – that microtubules show a robust astral organization. They mostly emanate from few and large MTOCs concentrated on the nucleus surface, and grow radially towards the cell cortex. Previous studies proposed that functional MTOCs assemble at the onset of the first meiotic M phase only, either *de novo* (Schuh and Ellenberg, 2007) or from inactive "centrosome precursors" (Calarco, 2000). The large and alveolated PCM foci we describe in competent oocytes act as predominant sites for microtubule nucleation, tether emanating microtubules and can thus be defined as functional MTOCs. Our data establish unambiguously the pre-existence of functional MTOCs in prophase-arrested oocytes. As a major differences with somatic centrosomes, the size and nucleation capacity of these flexible MTOCs, as well as their number per cell, are quite variable.

How do these acentriolar MTOCs form? Our data indicate that this process involves on one hand a quantitative change in the PCM foci. Starting with tiny nucleation sites, some of them being undetectable by immunostaining, the protracted growth phase associates with their gradual enlargement. The fact that the ratio of γ-tubulin and pericentrin of individual foci remains constant between growing and competent oocytes, may suggest that the increase in microtubule nucleation capacity could in a certain way depend on the increase in size of foci rather than on differential loading of γ-TURC (for γ-TUbulin Ring Complex), the functional unit for microtubule nucleation. In somatic cells, laser ablation of centrioles can lead to *de novo* canonical centrosome assembly. In this case, diffuse PCM initially form tiny foci that progressively aggregate to form larger structures (La Terra et al., 2005). In oocytes, existing foci could recruit dispersed material to self-organize larger and more robust structures. This process completed within few hours in somatic cells would take place in prophase arrested oocytes on a stretched time scale. Alternatively, composition of PCM may vary along oocyte growth such that key additional factors could contribute to the observed increase in MTOCs size and nucleation capacity.

The end of growth phase is marked by the repositioning of the nucleus towards the cell center (Brunet and Maro, 2007) and by the remodelling of the MTOC- microtubule network into large asters associated with the nucleus. In most systems, such radial organization serves to map the cell center and position the nucleus accordingly (Minc et al., 2011; Reinsch and Gonczy, 1998). Surprisingly, and in contrast to previous observations (Alexandre et al., 1989), we did not find any effect of microtubule depolymerization on nucleus position. In mouse oocytes, the role of F-actin in nucleus centering has been documented (Azoury et al., 2011; Dumont et al., 2007b). The cytoplasmic and perinuclear actin filaments may therefore likely fulfil this centration process.

The relevance of forming perinuclear microtubule asters focused on large and globular MTOCs in competent oocytes has to be sought after meiosis resumption, at the onset of the first meiotic division. Our data indicate that the nucleus is to some extent malleable, and that microtubules promote the formation of dynamic invaginations on its surface. Upon meiosis resumption, globular MTOCs expressly elongate. Microtubules remain tightly associated with the nuclear envelope, more precisely in invaginations that enlarge together with MTOCs elongation. The maintenance of one or few invaginations is associated with a global smoothening of the nucleus, indicative that the envelope is mechanically put under tension prior NEBD (Beaudouin et al., 2002). At that stage, MTOCs are the unique sites of microtubule nucleation and the actin meshwork that was present in prophase I is dismantled (Azoury et al., 2011): it is thus tempting to speculate that MTOC elongation drives the remodelling of nuclear envelope and mechanically prepares the nucleus and its underlying lamina meshwork (Combelles and Albertini, 2001) for its break-down.

The redistribution of perinuclear MTOCs along the nuclear envelope ends up by their even distribution around the chromosomes at NEBD. In somatic cells, the separation of centrosomes in prophase to opposite sides of the nucleus is beneficial for further chromosome segregation (Kaseda et al., 2012). Similarly, in mouse oocytes, forming a cage of dense microtubule nucleation centres around the chromosomes may facilitate chromosome capture, as shown in mitosis (Magidson et al., 2011). Therefore, gathering MTs-nucleation centers on the nucleus during oocyte growth in a first step to further distribute them evenly around the nucleus of competent oocytes may thus arise from a strategy developed in this acentriolar system to minimize the risk of chromosome loss in the large volume of the oocyte, to sort them more easily into two equal poles and thus prevent further aneuploidy of the gamete.

Funding

This work was supported by grants from the *Ligue Nationale Contre le Cancer* (EL2009/LNNCC/MHV and EL2012 /LNCC/MHV) and from the *Agence Nationale pour la Recherche* (ANR08-BLAN-0136-01 to MHV).

ML is recipient of PhD grant by the Émergence-UPMC 2010 research program.

Acknowledgements

We are grateful to M. Breuer and J. Dumont for critical reading of the manuscript and to the reviewers for their helpful comments.

Appendix A. Supporting information

Supplementary data associated with this article can be found in the online version at http://dx.doi.org/10.1016/j.ydbio.2013.07.029.

References

Alexandre, H., Van Cauwenberge, A., Mulnard, J., 1989. Involvement of microtubules and microfilaments in the control of the nuclear movement during maturation of mouse oocyte. Dev. Biol. 136, 311–320.

Azoury, J., Lee, K.W., Georget, V., Hikal, P., Verlhac, M.H., 2011. Symmetry breaking in mouse oocytes requires transient F-actin meshwork destabilization. Development 138, 2903–2908.

Azoury, J., Lee, K.W., Georget, V., Rassinier, P., Leader, B., Verlhac, M.H., 2008. Spindle positioning in mouse oocytes relies on a dynamic meshwork of actin filaments. Curr. Biol. 18, 1514–1519.

Beaudouin, J., Gerlich, D., Daigle, N., Eils, R., Ellenberg, J., 2002. Nuclear envelope breakdown proceeds by microtubule-induced tearing of the lamina. Cell 108, 83–96.

Bellone, M., Zuccotti, M., Redi, C.A., Garagna, S., 2009. The position of the germinal vesicle and the chromatin organization together provide a marker of the developmental competence of mouse antral oocytes. Reproduction 138, 639–643.

Bornens, M., 2008. Organelle positioning and cell polarity. Nat. Rev. Mol. Cell. Biol. 9, 874–886.

Breuer, M., Kolano, A., Kwon, M., Li, C.C., Tsai, T.F., Pellman, D., Brunet, S., Verlhac, M.H., 2010. HURP permits MTOC sorting for robust meiotic spindle bipolarity, similar to extra centrosome clustering in cancer cells. J. Cell Biol. 191, 1251–1260.

Brunet, S., Maria, A.S., Guillaud, P., Dujardin, D., Kubiak, J.Z., Maro, B., 1999. Kinetochore fibers are not involved in the formation of the first meiotic spindle in mouse oocytes, but control the exit from the first meiotic M phase. J. Cell Biol. 146, 1–12.

Brunet, S., Maro, B., 2007. Germinal vesicle position and meiotic maturation in mouse oocyte. Reproduction 133, 1069–1072.

Brunet, S., Verlhac, M.H., 2011. Positioning to get out of meiosis: the asymmetry of division. Hum. Reprod. Update 17, 68–75.

Burkel, B.M., von Dassow, G., Bement, W.M., 2007. Versatile fluorescent probes for actin filaments based on the actin-binding domain of utrophin. Cell. Motil. Cytoskeleton 64, 822–832.

Calarco, P.G., 2000. Centrosome precursors in the acentriolar mouse oocyte. Microsc. Res. Tech. 49, 428–434.
Can, A., Semiz, O., Cinar, O., 2003. Centrosome and microtubule dynamics during early stages of meiosis in mouse oocytes. Mol. Hum. Reprod. 9, 749–756.
Carabatsos, M.J., Combelles, C.M., Messinger, S.M., Albertini, D.F., 2000. Sorting and reorganization of centrosomes during oocyte maturation in the mouse. Microsc. Res. Tech. 49, 435–444.
Combelles, C.M., Albertini, D.F., 2001. Microtubule patterning during meiotic maturation in mouse oocytes is determined by cell cycle-specific sorting and redistribution of gamma-tubulin. Dev. Biol. 239, 281–294.
Desai, A., Mitchison, T.J., 1997. Microtubule polymerization dynamics. Annu. Rev. Cell. Dev. Biol. 13, 83–117.
Dumont, J., Desai, A., 2012. Acentrosomal spindle assembly and chromosome segregation during oocyte meiosis. Trends Cell. Biol.
Dumont, J., Petri, S., Pellegrin, F., Terret, M.-E., Bohnsack, M.T., Rassinier, P., Georget, V., Kalab, P., Gruss, O.J., Verlhac, M.-H., 2007a. A centriole and RanGTP independent spindle assembly pathway in meiosis I of vertebrate oocytes. J. Cell Biol. 176, 295–305.
Dumont, J., Million, K., Sunderland, K., Rassinier, P., Lim, H., Leader, B., Verlhac, M.H., 2007b. Formin-2 is required for spindle migration and for the late steps of cytokinesis in mouse oocytes. Dev. Biol. 301, 254–265.
Edson, M.A., Nagaraja, A.K., Matzuk, M.M., 2009. The mammalian ovary from genesis to revelation. Endocr. Rev. 30, 624–712.
Firestone, A.J., Weinger, J.S., Maldonado, M., Barlan, K., Langston, L.D., O'Donnell, M., Gelfand, V.I., Kapoor, T.M., Chen, J.K., 2012. Small-molecule inhibitors of the AAA+ ATPase motor cytoplasmic dynein. Nature 484, 125–129.
Gueth-Hallonet, C., Antony, C., Aghion, J., Santa-Maria, A., Lajoie-Mazenc, I., Wright, M., Maro, B., 1993. gamma-Tubulin is present in acentriolar MTOCs during early mouse development. J. Cell. Sci. 105 (Pt 1), 157–166.
Hertig, A.T., Adams, E.C., 1967. Studies on the human oocyte and its follicle. I. Ultrastructural and histochemical observations on the primordial follicle stage. J. Cell Biol. 34, 647–675.
Kalab, P., Weis, K., Heald, R., 2002. Visualization of a Ran-GTP gradient in interphase and mitotic Xenopus egg extracts. Science 295, 2452–2456.
Kaseda, K., McAinsh, A.D., Cross, R.A., 2012. Dual pathway spindle assembly increases both the speed and the fidelity of mitosis. Biol. Open 1, 12–18.
Kolano, A., Brunet, S., Silk, A.D., Cleveland, D.W., Verlhac, M.H., 2012. Error-prone mammalian female meiosis from silencing the spindle assembly checkpoint without normal interkinetochore tension. Proc. Natl. Acad. Sci. USA.
Krarup, T., Pedersen, T., Faber, M., 1969. Regulation of oocyte growth in the mouse ovary. Nature 224, 187–188.
La Terra, S., English, C.N., Hergert, P., McEwen, B.F., Sluder, G., Khodjakov, A., 2005. The de novo centriole assembly pathway in HeLa cells: cell cycle progression and centriole assembly/maturation. J. Cell Biol. 168, 713–722.
Magidson, V., O'Connell, C.B., Loncarek, J., Paul, R., Mogilner, A., Khodjakov, A., 2011. The spatial arrangement of chromosomes during prometaphase facilitates spindle assembly. Cell 146, 555–567.
Manandhar, G., Schatten, H., Sutovsky, P., 2005. Centrosome reduction during gametogenesis and its significance. Biol. Reprod. 72, 2–13.
Maro, B., Howlett, S.K., Webb, M., 1985. Non-spindle microtubule organizing centers in metaphase II-arrested mouse oocytes. J. Cell Biol. 101, 1665–1672.
Mattson, B.A., Albertini, D.F., 1990. Oogenesis: chromatin and microtubule dynamics during meiotic prophase. Mol. Reprod. Dev. 25, 374–383.
Minc, N., Burgess, D., Chang, F., 2011. Influence of cell geometry on division-plane positioning. Cell 144, 414–426.
Reinsch, S., Gonczy, P., 1998. Mechanisms of nuclear positioning. J. Cell. Sci. 111 (Pt 16), 2283–2295.
Schuh, M., Ellenberg, J., 2007. Self-organization of MTOCs replaces centrosome function during acentrosomal spindle assembly in live mouse oocytes. Cell 130, 484–498.
Sorensen, R.A., Wassarman, P.M., 1976. Relationship between growth and meiotic maturation of the mouse oocyte. Dev. Biol. 50, 531–536.
Stepanova, T., Slemmer, J., Hoogenraad, C.C., Lansbergen, G., Dortland, B., De Zeeuw, C.I., Grosveld, F., van Cappellen, G., Akhmanova, A., Galjart, N., 2003. Visualization of microtubule growth in cultured neurons via the use of EB3-GFP (end-binding protein 3-green fluorescent protein). J. Neurosci. 23, 2655–2664.
Szollosi, D., Calarco, P., Donahue, R.P., 1972. Absence of centrioles in the first and second meiotic spindles of mouse oocytes. J. Cell. Sci. 11, 521–541.
Thery, M., Bornens, M., 2006. Cell shape and cell division. Curr. Opin. Cell. Biol. 18, 648–657.
Tsurumi, C., Hoffmann, S., Geley, S., Graeser, R., Polanski, Z., 2004. The spindle assembly checkpoint is not essential for CSF arrest of mouse oocytes. J. Cell Biol. 167, 1037–1050.
Verde, F., Berrez, J.M., Antony, C., Karsenti, E., 1991. Taxol-induced microtubule asters in mitotic extracts of Xenopus eggs: requirement for phosphorylated factors and cytoplasmic dynein. J. Cell Biol. 112, 1177–1187.
Verlhac, M.H., Lefebvre, C., Guillaud, P., Rassinier, P., Maro, B., 2000. Asymmetric division in mouse oocytes: with or without Mos. Curr. Biol. 10, 1303–1306.
Zhao, T., Graham, O.S., Raposo St, A., Johnston, D., 2012. Growing microtubules push the oocyte nucleus to polarize the Drosophila dorsal-ventral axis. Science 336, 999–1003.